

miRNA-96 Suppresses KRAS and Functions as a Tumor Suppressor Gene in Pancreatic Cancer

Shuangni Yu¹, Zhaohui Lu¹, Changzheng Liu², Yunxiao Meng¹, Yihui Ma¹, Wugan Zhao¹, Jianping Liu¹, Jia Yu^{2,3}, and Jie Chen¹

Abstract

Therapeutic applications of microRNA (miRNA) in KRAS-driven pancreatic cancers might be valuable, but few studies have explored this area. Here, we report that miR-96 directly targets the *KRAS* oncogene and functions as a tumor-suppressing miRNA in pancreatic cancer cells. Ectopic expression of miR-96 through a synthetic miRNA precursor inhibited KRAS, dampened Akt signaling, and triggered apoptosis in cells. In human clinical specimens, miR-96 was downregulated or deleted where an association with KRAS elevations was observed. *In vitro* and *in vivo* assays established that miR-96 decreased cancer cell invasion and migration and slowed tumor growth in a manner associated with KRAS downregulation. Our findings identify miR-96 as a potent regulator of KRAS, which may provide a novel therapeutic strategy for treatment of pancreatic cancer and other KRAS-driven cancers. *Cancer Res*; 70(14); 6015–25. ©2010 AACR.

Introduction

MicroRNAs (miRNA) have drawn more attention than the other classes of noncoding RNAs in the past several years, especially for their essential roles in cancer. More than 50% of the known miRNAs have been shown to participate in human tumorigenesis and/or metastasis by directly targeting oncogenes or tumor suppressor genes (1, 2). For example, a miR-17-92 cluster was found to be located in a region that is commonly amplified in multiple human cancers. One of its targets is E2F, a transcription factor that is associated with DNA replication and apoptosis (3). MiR-21 could accelerate tumorigenesis by targeting several tumor suppressor genes, such as *PTEN*, *TMI*, and *PDCD4* (4, 5). In contrast, several miRNAs have been indicated to target oncogenes in tumors, such as miR-15/16 targeting *BCL2* in chronic lymphocytic leukemia (6), let-7 targeting *RAS* in lung cancer (7), miR-125a/125b targeting *ERBB2* and *ERBB3* in ovarian cancer (8), and miR-145 targeting

c-Myc in colon cancer (9). Dysregulation of these miRNAs may directly lead to subsequent abnormal expression of their targets, resulting in tumorigenesis.

KRAS is one of the three members of the *RAS* oncogene family, which encode small GTPases that are involved in cellular signal transduction (10). Activation of RAS signaling causes cell growth, differentiation, and survival. Moreover, activation of *KRAS* oncogene has been implicated in more than 90% of pancreatic carcinogenesis, and KRAS mutation represents one of the earliest genetic alterations in pancreatic cancer development (11–13). Oncogenic KRAS promotes pancreatic tumorigenesis through activation of multiple downstream pathways, including phosphatidylinositol 3-kinase (PI3K)/Akt, extracellular signal-regulated kinase (ERK), Bad, and NF- κ B (14–18). KRAS downregulation could reduce tumor growth and enhance gemcitabine chemotherapy efficacy for pancreatic cancer treatment. Thus, KRAS silencing has become an efficient therapeutic strategy in pancreatic cancer and other KRAS-driven cancers, but it is still far from optimal and novel therapeutic strategies are needed urgently.

In our recent work using a miRNA microarray observed that miR-96 is strongly downregulated (more than 5-fold) in pancreatic cancer versus normal tissue (19). Our data provided a solid proof for miR-96 expression in pancreatic cancer patients and indicated that it may play a role as a tumor suppressor in human pancreatic cancer progression. Then, we confirmed that miR-96 directly targets KRAS and showed the antiproliferative, proapoptotic, and antimetastatic properties of miR-96 by a subset of *in vitro* assays. To understand how miR-96 controls cell phenotypes by targeting KRAS, we then conducted a series of rescue assays and showed that miR-96 could negatively regulate the phosphorylated Akt (P-Akt) signaling pathway downstream of KRAS. Finally, xenograft models were used to assess the antiproliferation effect of miR-96. Expectedly, introduction of miR-96 significantly

Authors' Affiliations: ¹Department of Pathology, Peking Union Medical College Hospital, and ²Department of Biochemistry, National Laboratory of Medical Molecular Biology, Institute of Basic Medical Sciences, Chinese Academy of Medical Sciences and Peking Union Medical College, Tsinghua University, Beijing, PR China; and ³Department of Dermatology, Feinberg School of Medicine, Northwestern University, Chicago, Illinois

Note: Supplementary data for this article are available at Cancer Research Online (<http://cancerres.aacrjournals.org/>).

Corresponding Authors: Jie Chen, Department of Pathology, Peking Union Medical College Hospital, Chinese Academy of Medical Sciences and Peking Union Medical College, Tsinghua University, Beijing 100730, PR China. Phone: 86-010-65295490; Fax: 86-010-65295490; E-mail: xhblk@163.com; Jia Yu, Department of Biochemistry, National Laboratory of Medical Molecular Biology, Institute of Basic Medical Sciences, Chinese Academy of Medical Sciences and Peking Union Medical College, Beijing 100005, PR China. Phone: 86-010-65296433; Fax: 86-010-65296433; E-mail: j-yu@ibms.pumc.edu.cn.

doi: 10.1158/0008-5472.CAN-09-4531

©2010 American Association for Cancer Research.

inhibited the tumorigenicity of pancreatic cancer cells in these nude mouse models.

These results provide insights into our understanding of how one miRNA acts as a tumor suppressor and suggest a novel therapeutic strategy for treatment of pancreatic cancer and other KRAS-driven cancers.

Materials and Methods

Human tissue samples and cell lines

Tissues were obtained from patients undergoing surgery for pancreatic cancer in Peking Union Hospital, immediately snap-frozen in liquid nitrogen, and stored at -80°C until RNA extraction. The characteristics of patients included are described in Supplementary Table S1. The pancreatic cancer cell lines MIA PaCa-2, PANC-1, and BxPC-3 and the cervical adenocarcinoma cell line HeLa were obtained from the American Type Culture Collection in 1999 and cultured in DMEM (Sigma) supplemented with 10% fetal bovine serum (FBS; Hyclone) at 37°C with 5% CO_2 . These cell lines were tested 1 month before the experiment by methods of morphology check by microscopy, growth curve analysis, and *Mycoplasma* detection according to the ATCC cell line verification test recommendations.

Quantification of RNA and protein

Total RNA was extracted from the cells and tissues with TRIzol reagent (Invitrogen). Real-time reverse transcription-PCR assay was conducted to detect the mRNA levels of KRAS and glyceraldehyde-3-phosphate dehydrogenase (GAPDH). Northern blotting analysis of miRNAs and Western blotting of protein were performed as described previously (20). Probes were labeled with $[\gamma\text{-}^{32}\text{P}]\text{ATP}$ complementary to miR-96 and U6 snRNA. The antibodies included those against ERK, phosphorylated ERK (P-ERK), Akt, P-Akt, Bad, phosphorylated Bad, KRAS, and β -actin (KRAS and β -actin from Santa Cruz, others from CST).

Constructs, transfections, and assays

The 3' untranslated region (3'-UTR) of human KRAS mRNA was cloned in between the *Not*I and *Xba*I sites of pRL-TK (Promega) using PCR-generated fragment. Mutation of the KRAS sequence was created using a Quick-Change Site-Directed Mutagenesis kit (Stratagene). The miR-96 miRNA precursor (pre-miR-96) and a control precursor (scramble) were purchased from Ambion, Inc. A miR-96 expression plasmid (pcDNAmiR-96) was constructed using synthetic oligonucleotides and the pcDNA6.2-GW/EmGFP vector. The KRAS expression plasmid (pcDNA3.1KRAS) was made using pcDNA3.1 vector and PCR-generated fragment from genome.

HeLa, MIA PaCa-2, and PANC-1 cells were seeded onto 24-well plates (1×10^5 cells per well) the day before transfections were performed. Cells ($\sim 70\%$ confluent) were transfected with pRL-TK luciferase reporters (50 ng/well), pGL-3 firefly luciferase (10 ng/well), and pre-miR-96 (50 nmol/L) or scramble (50 nmol/L) using Lipofectamine 2000 (Invitrogen).

Luciferase activities were measured using the Dual Luciferase Reporter Assay (Promega).

For Western blotting and other functional analyses, pre-miR-96 or scramble was transfected into MIA PaCa-2 and PANC-1 cells (50 nmol/L) by using Lipofectamine 2000. pcDNAmiR-96 or control vector was transfected (2 $\mu\text{g}/\text{mL}$) into MIA PaCa-2 cells using Lipofectamine 2000, and stable miR-96-expressing cells were selected with antibiotic. For the miRNA and pcDNA3.1KRAS combination experiments, MIA PaCa-2 cells were grown in normal culture medium containing 50 nmol/L pre-miR-96 or scramble for 24 hours. These cells were then cotreated with different combinations of 2 $\mu\text{g}/\text{mL}$ pcDNA3.1 construct (KRAS or empty) and 50 nmol/L oligonucleotide (pre-miR-96 or scramble) for another 24 hours. pcDNA3.1KRAS transfection 24 hours before pre-miR-96 or cotransfection was also performed.

Cell proliferation, apoptosis, and cell cycle assay

Cells were incubated in 10% CCK-8 (DOJINDO) diluted in normal culture medium at 37°C until visual color conversion occurred. Proliferation rates were determined at 24, 48, 72, 96, 120, or 144 hours after transfection.

The apoptosis assay was performed on MIA PaCa-2 and PANC-1 cell lines 48 or 72 hours after transfection using the Annexin V-FITC Apoptosis Detection Kit I (BD Biosciences) and analyzed by fluorescence-activated cell sorting (FACS).

Cell cycle analysis was performed on MIA PaCa-2 and PANC-1 cells 72 hours after transfection with either pre-miR-96 or scramble. Cells were trypsinized and collected after being washed with PBS twice, fixed in 70% cold ethanol, and incubated with propidium iodide (PI), then analyzed by FACS.

Soft-agar colony formation, cell migration, and invasion assays

A 1.5-mL base layer of agar (0.5% agar in DMEM with 10% FBS) was allowed to solidify in a six-well flat-bottomed plate before the addition of 1.5 mL of cell suspensions containing 4,000 cells in 0.35% agar in DMEM with 10% FBS. The cell-containing layer was then solidified at 4°C for 20 minutes. Colonies were allowed to grow for 21 days at 37°C with 5% CO_2 before imaging.

A wound-healing assay was done to assess cell migration. An artificial wound was created 24 hours after transfection using a 200- μL pipette tip on the confluent cell monolayer and mitomycin C was added to the culture wells (final concentration for PANC-1, 10 $\mu\text{g}/\text{mL}$; for MIA PaCa-2, 20 $\mu\text{g}/\text{mL}$). To visualize migrated cells and wound healing, images were taken at 0, 12, 24, 36, 48, and 60 hours.

Invasion assay was evaluated by the ability of cells passing through Matrigel-coated membrane matrix (BD Biosciences). Cells were seeded onto a Matrigel-coated membrane matrix present in the insert of a 24-well culture plate 24 hours after transfection. Fetal bovine serum was added to the lower chamber as a chemoattractant. After 24 hours, the noninvading cells were removed. Invasive cells located on the lower surface of the chamber were stained with 0.1% crystal violet (Sigma) and counted.

Pancreatic tumor xenograft model

Six-week-old male nude mice (BALB/c-nude) were used to examine tumorigenicity. MIA PaCa-2 stable cells overexpressing miR-96 or vector control cells were propagated and 6×10^6 cells were inoculated s.c. into the dorsal flanks of 18 mice (5 for wild-type, 5 for vector control, and 8 for stably overexpressing miR-96). Tumor size was measured every week, and tumor volumes were estimated. For end-point experiments, tumors were removed and weighed 7 weeks after tumor cell injection.

Immunohistochemistry

Mouse tumor tissues were made into paraffin sections and pretreated at 65°C for 2 hours, followed by deparaffinization. Antigen retrieval was carried out before application of the primary antibodies [KRAS, Ki-67, and p53 (mutated); 1:100; DAKO] overnight at 4°C. As a negative control, sections were incubated with normal IgG. Thereafter, slides were incubated for 2 hours at room temperature with the secondary antibody conjugated to horseradish peroxidase (HRP; 1:100; DAKO). HRP activity was detected using the Liquid DAB+ Substrate Chromogen System (DAKO). Finally, sections were counterstained with hematoxylin and photographed.

Statistics

Each experiment was repeated at least three times. Student's *t* test (two-tailed) was performed, and statistical significance level was set at $\alpha = 0.05$ (two-side). Mean \pm SD is displayed in the figures.

Results and Discussion

Aberrant miR-96 expression in pancreatic cancer

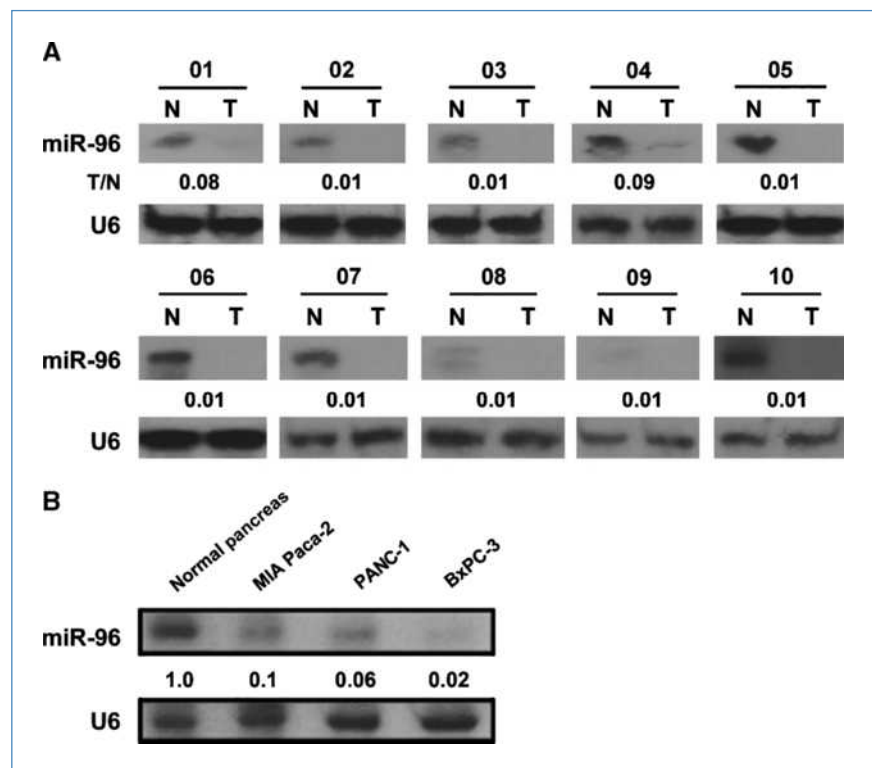
To assess the expression of miR-96 in pancreatic cancer, Northern blotting analysis was conducted in 10 pairs of pancreatic cancer tissue and matched adjacent normal tissue samples. The expression of miR-96 was consistently lower in the pancreatic cancer tissues than in normal tissues (Fig. 1A). Furthermore, analysis of miR-96 expression in three pancreatic cancer cell lines (MIA PaCa-2, PANC-1, and BxPC-3), revealed that miR-96 was downregulated in tumor cell lines as well (Fig. 1B). These data support the notion that miR-96 may act as a tumor suppressor in pancreatic cancer.

KRAS is a direct target of miR-96

To fully understand the mechanisms by which miRNAs execute their function, we adopted three bioinformatic algorithms (TargetScan, PicTar, and miRanda) to identify a large number of potential target genes of miR-96. Among these candidates, KRAS was selected for further analysis. A binding site of miR-96 was observed in the 3'-UTR of KRAS mRNA. Moreover, there was perfect base pairing between the "seed sequence" of mature miR-96 and its cognate targets (including KRAS), and the seed sequences were exactly conserved across species (Fig. 2A).

To test the hypothesis that KRAS might be a target of miR-96, a reporter plasmid harboring the wild-type 3'-UTR region of KRAS downstream of the luciferase coding region

Figure 1. miR-96 is downregulated in pancreatic cancer tissues and cell lines. Northern blotting analysis using a miR-96-specific probe showed the level of miR-96 (A) in 10 pairs of pancreatic cancer tissues (T) compared with matching controls (N; the patient numbers are indicated at the top) and (B) in the pancreatic cancer cell lines. The signal in each lane was quantified and the ratio of miR-96 to U6 snRNA was determined.



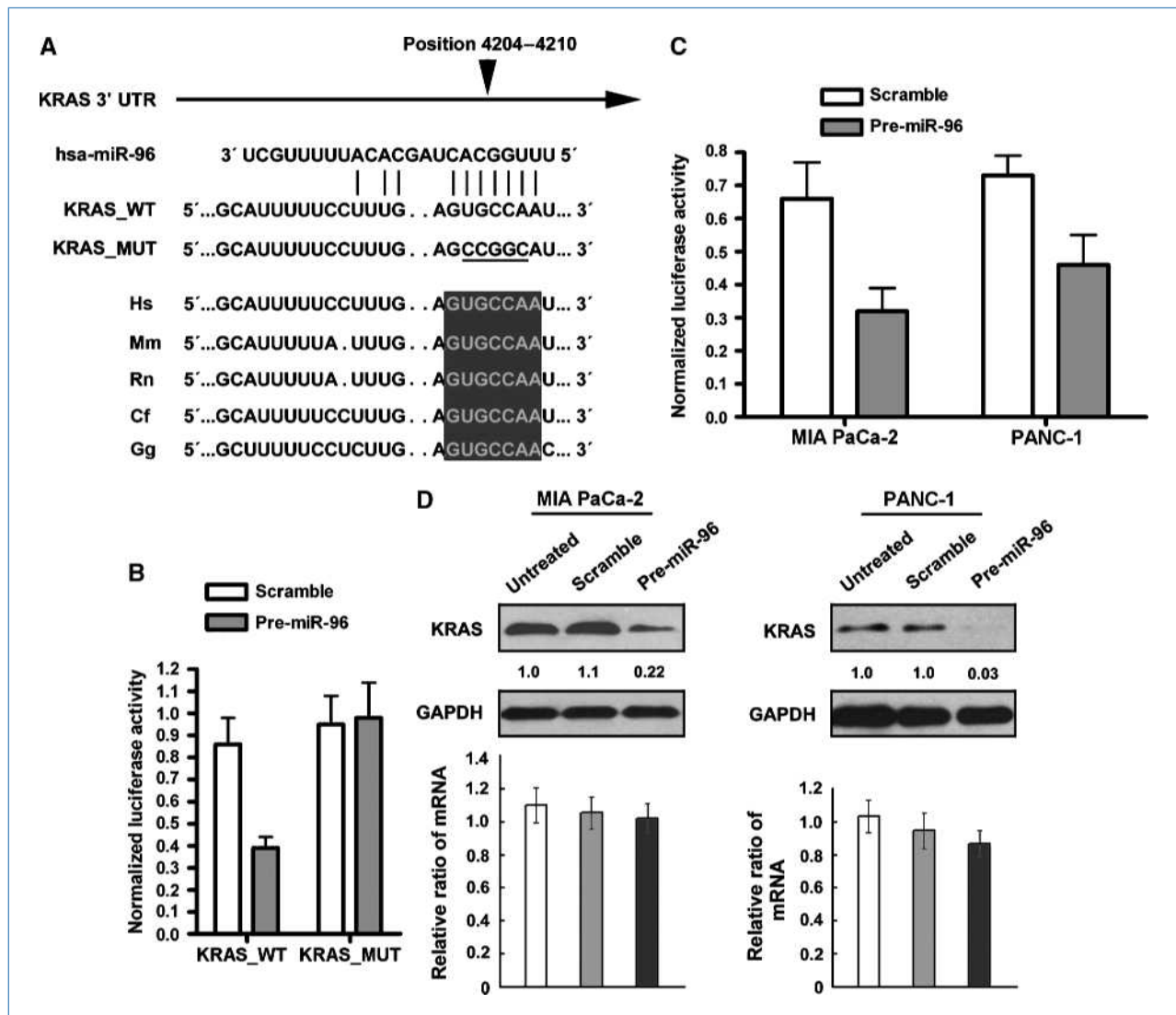


Figure 2. KRAS is experimentally validated as a direct target of miR-96 in pancreatic cancer cells. **A**, sequence of the miR-96 binding sites within the human KRAS 3'-UTR and a schematic diagram of the reporter constructs showing the entire KRAS 3'-UTR sequence (KRAS_WT) and the mutated KRAS 3'-UTR sequence (KRAS_MUT; the mutant nucleotides of the miR-96 binding site are underlined). Shaded areas represent conserved complementary nucleotides of the miR-96 seed sequence in various mammals (Hs, human; Mm, mouse; Rn, rat; Cf, chicken; Gg, goat). **B**, luciferase activity of the KRAS_WT reporter and the KRAS_MUT reporter in the presence of 10 nmol/L of pre-miR-96 or scramble. **C**, luciferase reporter assay of KRAS_WT in MIA PaCa-2 and PANC-1 cells in the presence of 10 nmol/L of pre-miR-96 or scramble. **D**, immunoblotting of KRAS in MIA PaCa-2 and PANC-1 cells not transfected or transfected with pre-miR-96 or scramble. The signal in each lane was quantified and the ratio of KRAS to GAPDH was determined. The relative expression of KRAS using real-time PCR was analyzed. GAPDH was used as a housekeeping control. All data are shown as mean \pm SD.

(Fig. 2A, KRAS_WT) was constructed. HeLa cells were cotransfected with reporter plasmid (KRAS_WT) and pre-miR-96/scramble. As a result, pre-miR-96-transfected cells showed a marked reduction ($\approx 56\%$) of luciferase activity (Fig. 2B). Then, the same assay was performed for another reporter plasmid containing mutated KRAS 3'-UTR in miR-96 binding sites (Fig. 2A, KRAS_MUT). As expected, the inhibition of luciferase activity by pre-miR-96 was almost abolished in the KRAS_MUT mutant, suggesting that the conserved region was fully responsible for miR-96 function (Fig. 2B).

MIA PaCa-2 and PANC-1 cells express low endogenous levels of miR-96 (Fig. 1B) and readily detectable levels of KRAS (21). The most straightforward prediction from our luciferase reporter assays would be that ectopic expression of miR-96 should reduce KRAS protein levels in MIA PaCa-2 and PANC-1 cells. To further investigate the interaction between miR-96 and KRAS, MIA PaCa-2 and PANC-1 cells were transfected with pre-miR-96. After a functional pre-miR-96 transfection test in MIA PaCa-2 and PANC-1 cells (Fig. 2C), Western blotting analysis was conducted to measure the level of KRAS protein. We found that the expression of KRAS

protein was downregulated in pre-miR-96-treated MIA PaCa-2/PANC-1 cells, but not in scramble or untreated cells (Fig. 2D). In addition, KRAS mRNA expression was determined by real-time PCR. We observed no significant differences between pre-miR-96-treated and scramble-treated or untreated MIA PaCa-2/PANC-1 cells (Fig. 2D). These data suggest that miR-96 directly recognizes the 3'-UTR of KRAS mRNA and inhibits KRAS translation. Thus, downregulated miR-96 in pancreatic cancer inhibits the suppression of KRAS, which in turn accelerates tumorigenesis.

Overexpression of miR-96 in pancreatic cancer cells inhibits cell proliferation, migration, and invasion

Given that KRAS plays a role in the regulation of cell proliferation and cell cycle, and that KRAS is able to increase the S-phase cell population (22), MIA PaCa-2 and PANC-1 cells were respectively transfected with pre-miR-96 or scramble and analyzed for cell growth and cell cycle progression. The CCK-8 proliferation assay showed that cell growth was reduced in pre-miR-96-transfected MIA PaCa-2 and PANC-1 cells compared with scramble-transfected cells or untreated cells (Fig. 3A). The cell cycle analysis further confirmed this observation, indicating that pre-miR-96 treatment induced cell cycle arrest in G₁ phase with a significant increase in the percentage of cells in G₁ phase (~21% in MIA PaCa-2 or ~10% in PANC-1) and a reduction of the S-phase cell population by ~18% (MIA PaCa-2) or ~7% (PANC-1; Fig. 3B). These results suggest that miR-96 could regulate cell proliferation by targeting KRAS. To further detect whether miR-96 is associated with progression of pancreatic cancer, we analyzed the effect of miR-96 expression on the migratory and invasive behavior of MIA PaCa-2 and PANC-1 cells. We found that introduction of miR-96 into MIA PaCa-2 and PANC-1 cells resulted in a significant reduction of cell migration during the closing of an artificial wound created over a confluent monolayer (Fig. 3C; Supplementary Fig. S1). Moreover, these cells were treated with mitomycin C during the course of wound healing to ensure that any augmented migratory behavior could not be affected by altered cell proliferation. In addition, restoration of miR-96 dramatically inhibited the normally strong invasive capacity of MIA PaCa-2 and PANC-1 cell lines, which carry low endogenous levels of miR-96 (Fig. 3D). These results show that miR-96 overexpression contributes to regulation of pancreatic cancer cell motility and progression *in vitro*.

Overexpression of miR-96 dampens the Akt signaling pathway

Activation of the KRAS pathway has been well documented in various tumor types, such as lung cancer (23, 24), breast cancer (25), colon cancer (26), and pancreatic cancer (27). Previous studies have shown the importance of the KRAS/Akt signaling pathway in the regulation of cell proliferation and survival in pancreatic cancer cells (28–30). To investigate whether miR-96 affected cell survival through the Akt pathway, we examined the phosphorylation level of Akt in MIA PaCa-2 and PANC-1 cells overexpressing miR-96. Cellular levels of P-Akt were significantly decreased

in pre-miR-96-transfected cells as compared with scramble-transfected or untreated cells (Fig. 4A). One consequence of Akt signaling alterations is an effect on cell survival (31). To address whether the lower levels of P-Akt resulting from the upregulation of miR-96 would induce pancreatic cancer cell apoptosis and cell death, we determined the number of early and late apoptotic MIA PaCa-2 and PANC-1 cells following treatment with pre-miR-96. As expected, few early apoptotic cells (17% in MIA PaCa-2 or 17.9% in PANC-1) were detected in the scramble-treated cells, whereas pre-miR-96 treatment increased the percentage of early apoptotic cells (41% in MIA PaCa-2 or 24.5% in PANC-1) as judged by Annexin V staining (Fig. 4B). Therefore, we concluded that miR-96 could directly target KRAS and subsequently affect cell survival through the Akt signaling pathway in pancreatic cancer cells.

Mutations of the *KRAS* gene are some of the earliest and most frequent genetic events observed in pancreatic cancer patients and are responsible for more than 95% of tumors (11–13, 32, 33). These abnormalities result in constitutive activation and subsequent stimulation of downstream signal transduction pathways regulating cellular survival, proliferation, and invasion. The PI3K/Akt pathway acts as a major downstream effector of KRAS signaling, and several downstream factors such as ERK, Bad, Bcl-xl, and NF- κ B have been linked to the Akt pathway (34). The ERK pathway is primarily known for mitogenic signaling and modulation of cell proliferation in most model systems (35). Constitutive activation of ERK has been observed in multiple cancer types, including pancreatic cancer cells (36, 37). To investigate whether the repression of cell growth observed in miR-96-overexpressing cells was mediated through this pathway, we measured the level of P-ERK in MIA PaCa-2 and PANC-1 cells after pre-miR-96 treatment. A significant decrease in P-ERK level was detected in pre-miR-96-treated cells compared with untreated and scramble-treated cells. However, no obvious difference was observed in total ERK level (Fig. 4A). These findings suggest that the accelerated pancreatic cancer cell growth was partially due to the overactivated Akt and ERK pathways.

Besides promoting cell proliferation, activated Akt could also phosphorylate Bad at Ser112 and Ser136 *in vitro* and *in vivo*, blocking Bad-induced cell death (16). In the absence of phosphorylation at these sites, Bad is thought to interact with Bcl-xl to induce cell death. In contrast, Akt-mediated hyperphosphorylation of Bad may promote cell survival in pancreatic cancer cells. Our Western blotting results confirmed the above speculation that the increased apoptosis in pre-miR-96-transfected cells was a result of decreased phosphorylation of Bad (Fig. 4A).

The fact that miR-96 was significantly downregulated in the majority of pancreatic cancer cells and that such a reduction was correlated with tumor progression suggests that endogenous miR-96 level may be an indicator of pancreatic cancer. Given that several miRNAs have been considered as potential tumor diagnostic markers, we believe that miR-96 might also be related to pancreatic malignancy diagnosis.

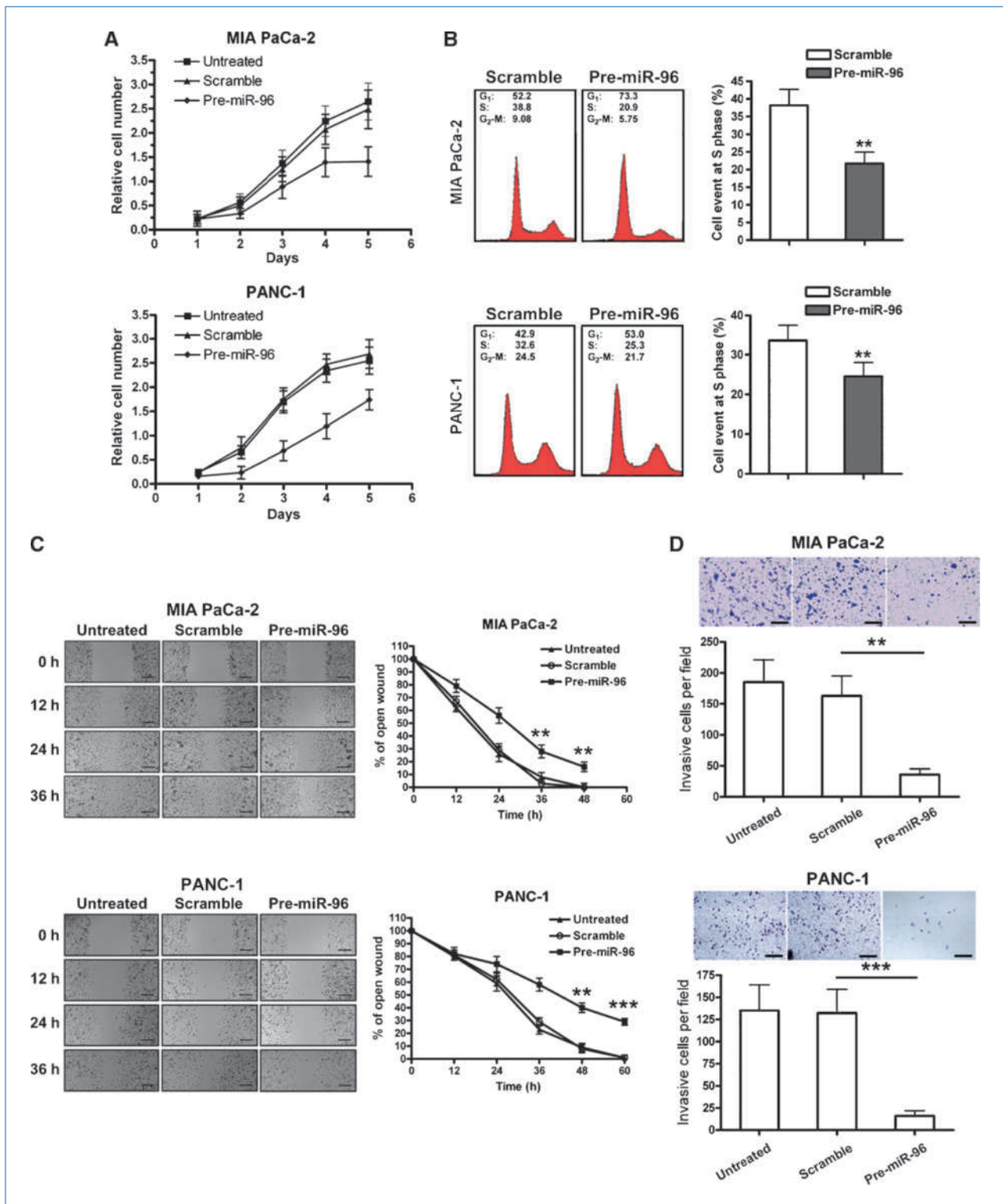


Figure 3. Overexpression of miR-96 inhibits pancreatic cancer cell growth, migration, and invasion *in vitro*. A, growth of MIA PaCa-2 and PANC-1 cells was shown after transfection with 50 nmol/L of pre-miR-96 or scramble or no transfection. The growth index was assessed at 1, 2, 3, 4, and 5 d. B, MIA PaCa-2 and PANC-1 were transfected with 50 nmol/L of pre-miR-96 or scramble for 72 h. C, MIA PaCa-2 and PANC-1 cells were not transfected or transfected with 50 nmol/L of pre-miR-96 or scramble for 24 h, and wounds were made. The relative ratio of wound closure per field is shown. D, MIA PaCa-2 and PANC-1 cells were not transfected or transfected with 50 nmol/L of pre-miR-96 or scramble for 24 h, and transwell invasion assay was performed. The relative ratio of invasive cells per field is shown. Magnification for identification of migration and invasion is $\times 60$. Bar, 100 μm . All data are shown as mean \pm SD. **, $P < 0.05$; ***, $P < 0.01$.

miR-96 affects pancreatic cancer cell proliferation, apoptosis, and migration by directly targeting the KRAS/Akt pathway

As we showed above, overexpression of miR-96 inhibited cell proliferation and migration while promoting cell apoptosis in pancreatic cancer cells. We also validated KRAS as a direct target of miR-96. Therefore, we wondered whether the changes in cell phenotypes after miR-96 overexpression directly resulted from the downregulation of KRAS and its downstream pathways. To test this idea, we designed a group of experiments, which would regulate the cellular level of KRAS in different situations, and monitored the corresponding phenotype changes in pancreatic cancer cells.

MIA PaCa-2 cells were first transfected with pre-miR-96 and then cotreated with pre-miR-96 and KRAS-expressing vector (pcDNA3.1KRAS) 24 hours later. The previous transfection of miRNA offered a sufficient decrease in KRAS protein level. Theoretically, the decreased KRAS level resulting from miR-96 transfection could be partially rescued via the introduction of pcDNA3.1KRAS. As expected, the level of KRAS protein in lane 5 was significantly higher than that in lane 4 (Fig. 5A, left). In contrast, in MIA PaCa-2 cells transfected first with pcDNA3.1KRAS and then with pre-miR-96 after 24 hours, the KRAS level in lane 4 was lower than that in lane 3 (Fig. 5A, right). Interestingly, the phosphorylation level of Akt was altered similarly to the expression level of KRAS (Fig. 5A), that is, decreased P-Akt directed by miR-96

overexpression could be rescued by upregulation of KRAS, and increased P-Akt by KRAS also could be dampened by miR-96. Moreover, this was confirmed by the functional assays of cotransfection including proliferation, apoptosis, and migration (Fig. 5B–D). As shown in Fig. 5B, an increase in cell growth was observed in cells cotransfected with pre-miR-96 and pcDNA3.1KRAS compared with cells cotransfected with pre-miR-96 and pcDNA3.1, corresponding to the higher KRAS and P-Akt levels in lane 5 compared with lane 4 (Fig. 5A, left). On the other hand, cells cotreated with scramble and pcDNA3.1KRAS exhibited the greatest extent of cell proliferation (Fig. 5B), as well as the highest cellular KRAS level (data not shown). Furthermore, the percentage of early apoptotic cells was rescued in d group (17.3%) in comparison with c group (23.4%; Fig. 5C), coincident with the rescued KRAS and P-Akt levels in lane 5 compared with lane 4 (Fig. 5A, left). Similarly, the capacity of cell migration in d group was also rescued, corresponding to that in c group, the same as the changes in KRAS level (Fig. 5A). Based on these findings, we concluded that miR-96 could regulate pancreatic cancer cell proliferation, apoptosis, and migration by directly targeting the KRAS/Akt pathway.

miR-96 affects tumor cell growth *in vitro* and *in vivo*

The remarkable reduction of miR-96 expression in pancreatic cancer samples prompted us to explore the possible biological significance of miR-96 in tumorigenesis. First, colony

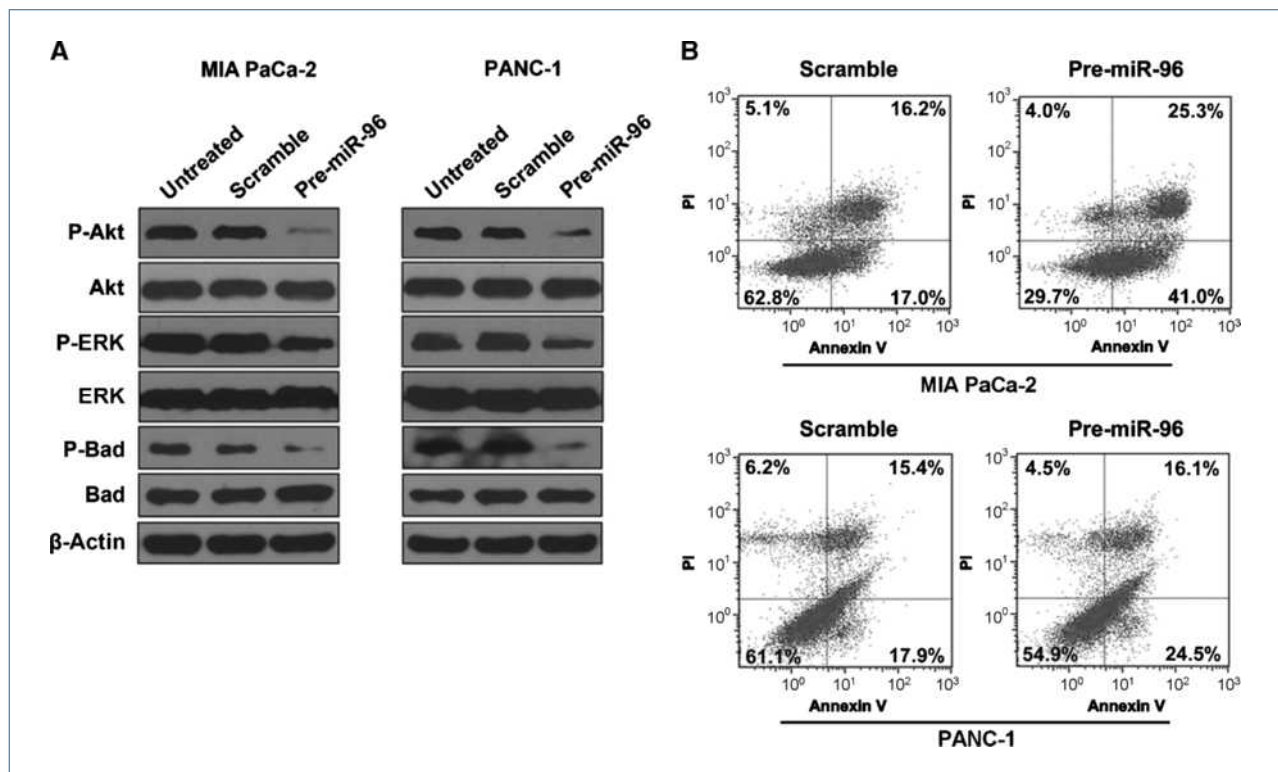


Figure 4. miR-96 affects the KRAS pathway and pancreatic cancer cell apoptosis. A, immunoblotting of P-Akt, Akt, P-ERK, ERK, P-Bad, and Bad in MIA PaCa-2 and PANC-1 cells not transfected or transfected with pre-miR-96 or scramble. β -Actin serves as a loading control. B, MIA PaCa-2 and PANC-1 cells were stained with PI and Annexin V 72 h after treatment with pre-miR-96 or scramble. Early and late apoptotic cells are shown in the right quadrant.

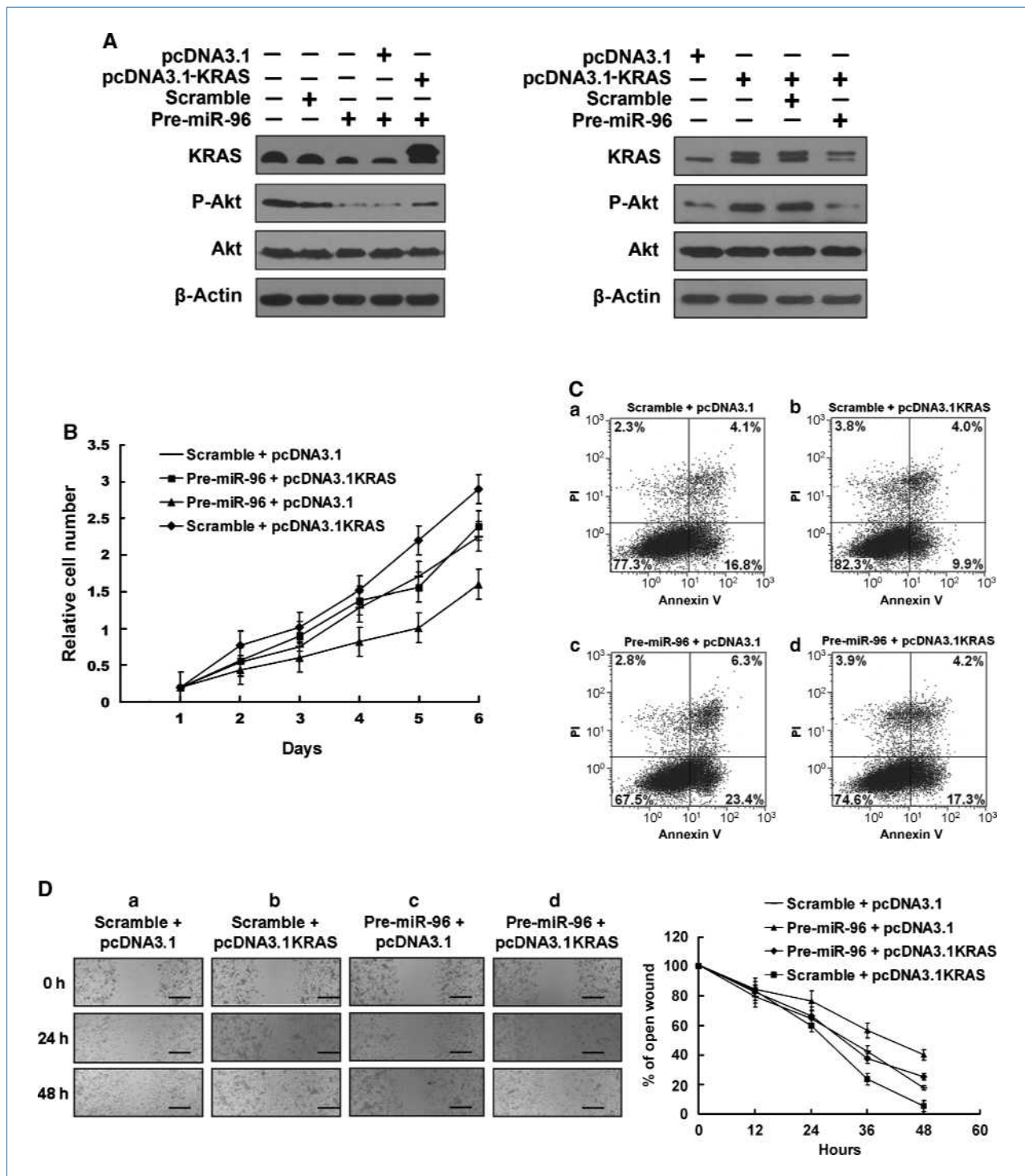


Figure 5. Functional assays of pre-miR-96 and pcDNA3.1KRAS cotransfection. A, KRAS and P-Akt protein levels were modulated by nontransfection, individual transfection with pre-miR-96 or scramble oligonucleotide, and cotransfection with one oligonucleotide and pcDNA3.1KRAS or pcDNA3.1. Left, pre-miR-96 was transfected 24 h before cotransfection with pcDNA3.1KRAS or pcDNA3.1 and pre-miR-96. Right, pcDNA3.1KRAS was transfected 24 h before cotransfection with pre-miR-96 or scramble oligonucleotide and pcDNA3.1KRAS. Immunoblotting of KRAS, P-Akt, and Akt in MIA PaCa-2 cells showed corresponding alterations. β -Actin served as a loading control. B, the growth of MIA PaCa-2 cells was measured in cells cotransfected with different combinations of pcDNA3.1 construct (KRAS or empty) and one oligonucleotide after 24-h treatment with one oligonucleotide (pre-miR-96 or scramble). The growth index was assessed at 1, 2, 3, 4, 5, and 6 d. C, MIA PaCa-2 cells were stained with PI and Annexin V after cotransfection as above. Early and late apoptotic cells are shown in the right quadrant. D, MIA PaCa-2 cells were treated as above, and wounds were made. Magnification for assessment of migration is $\times 60$. Bar, 100 μ m. The relative ratio of wound closure per field is shown. All data are shown as mean \pm SD.

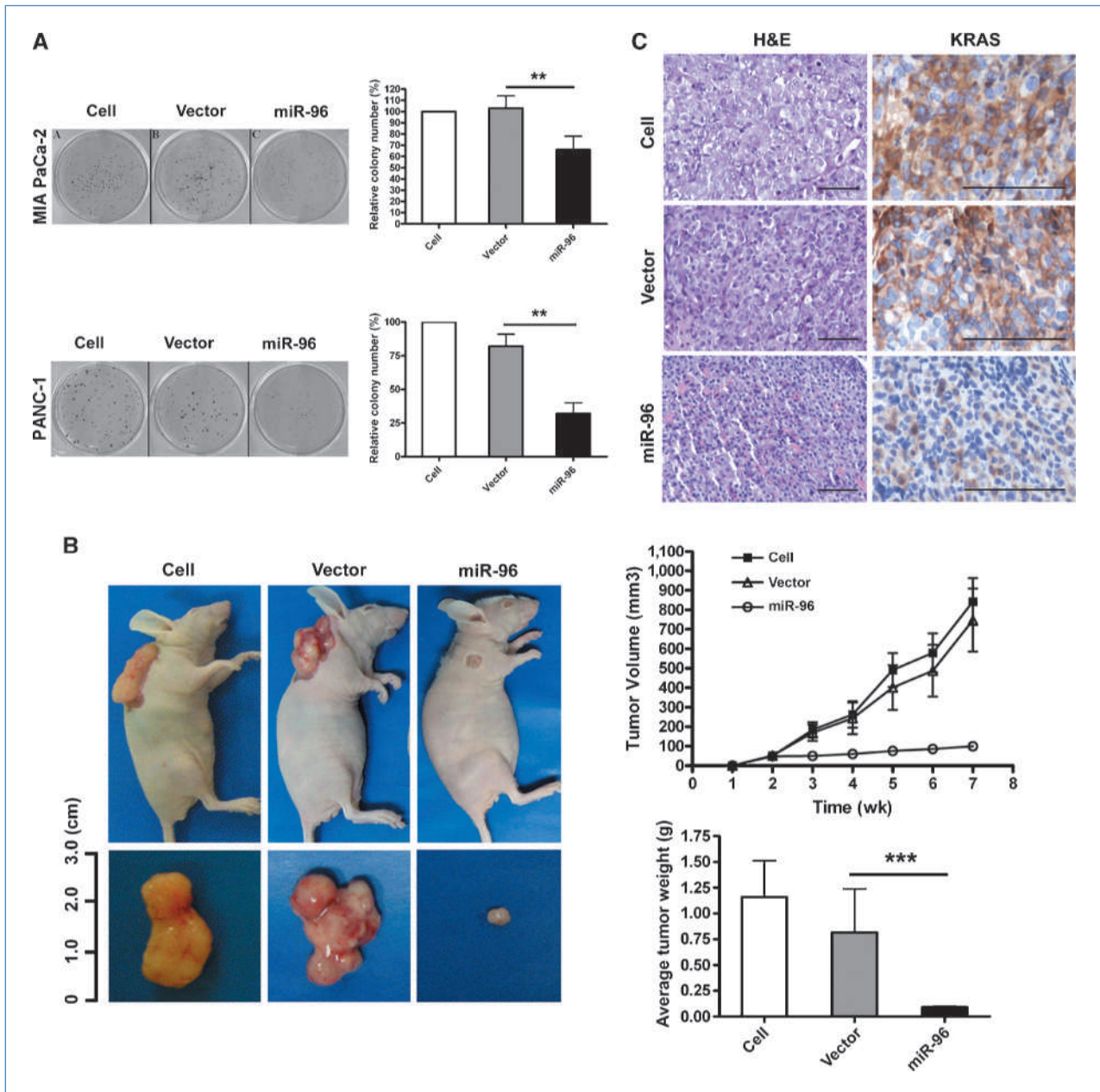


Figure 6. miR-96 inhibits tumor cell growth *in vitro* and *in vivo*. **A**, colony formation assay of untreated, scramble-transfected, and pre-miR-96-transfected MIA PaCa-2 and PANC-1 cells. All data are shown as mean \pm SD. **, $P < 0.05$. **B**, xenograft model in nude mice. Untreated, empty vector-transfected, and pcDNAmiR-96-transfected MIA PaCa-2 cells were injected s.c. into the posterior flank of nude mice. The graph is representative of tumor growth 7 wk after inoculation. Tumor volume and weight were calculated and all data are shown as mean \pm SD. **C**, expression of KRAS was measured by immunohistochemistry in the tissue extracted from pcDNAmiR-96, untreated, and empty vector mice. Magnification, $\times 60$ (H&E) and $\times 150$ (immunohistochemistry). Bar, 100 μ m.

formation experiments were performed to evaluate the growth capacity of pre-miR-96- or scramble-transfected or nontransfected pancreatic cancer cell lines (MIA PaCa-2 and PANC-1). As expected, pre-miR-96-transfected cells displayed fewer and smaller colonies compared with scramble-transfected and nontransfected cells (Fig. 6A). These data provide *in vitro* evidence of the growth-inhibitory role of miR-96.

To further verify the findings above, an *in vivo* model was also included. Untreated, empty vector-transfected, and pcDNAmiR-96-transfected MIA PaCa-2 cells were injected s.c. into the posterior flank of nude mice. After 7 weeks, we found that tumor growth was significantly slower in the miR-96-transfected mice than in the vector-treated and untreated controls (Fig. 6B; Supplementary Fig. S2). In

agreement with the tumor growth curve, the volumes of tumors induced by pcDNA_{miR-96}-transfected cells were significantly lower than those by the vector-treated and untreated controls (Fig. 6B). Moreover, we also performed immunohistochemistry to detect the expression of KRAS in randomly selected tumors derived from untreated, vector control-, or pcDNA_{miR-96}-transfected MIA PaCa-2 cells. The miR-96-overexpressing tumors expressed lower levels of KRAS than the others (Fig. 6C). In view of these observations, we reasoned that decreased levels of KRAS in mouse tumors after injection with pcDNA_{miR-96}-transfected MIA PaCa-2 cells might affect tumor cell proliferation. Similarly, immunohistochemical analysis was used to measure the protein levels of Ki-67 and mutated p53 in the tumor tissues, showing decreases of Ki-67 and mutated p53 in pcDNA_{miR-96}-transfected cell tissues (Supplementary Fig. S3). These data indicate that introduction of miR-96 remarkably inhibits the tumorigenicity of MIA PaCa-2 cells in the nude mouse xenograft model. Thus, miR-96 seems to regulate tumorigenesis through inhibition of proliferative and invasive activities by targeting KRAS. From a clinical standpoint, the possibility that introduction of miR-96 mimics (such as pre-miR-96) may contribute to pancreatic cancer control provides a novel method for pancreatic cancer therapy.

miRNAs, a novel class of regulatory molecules, have been frequently indicated to be often dysregulated in diverse human cancers (38, 39). miRNAs often act as oncogenes or tumor suppressors, regulating many cellular events. However, there are no results referring to the role of miR-96 in pancreatic cancer at present. One previous report indicated that miR-96 was upregulated in breast cancer, suggesting that it might have an oncogenic role (40). In our study, we confirmed that miR-96 acts as a tumor suppressor gene through various mechanisms, including inhibition of tumor cell

growth, migration, invasion, acceleration of cell apoptosis, and direct targeting of the KRAS/Akt signaling pathway. The discrepancy between our results and those of previous studies may be due to the differences in the systems used and the lack of further functional analysis of miR-96.

In summary, we have identified a link between miR-96 and KRAS that is a novel constituent of pancreatic cancer tumorigenesis. Over the past few years, it has been shown that the let-7 family and miR-143 target KRAS in tumors of different tissue origins such as lung, breast, and colon cancers. We speculate that these tissue-specific miRNAs may contribute to the cognate abnormality via similar pathways.

Disclosure of Potential Conflicts of Interest

No potential conflicts of interest were disclosed.

Acknowledgments

We thank Dr. Tonghua Liu (pcDNA6.2-GW/EmGFP) and Dr. Qiang Zhang (pcDNA3.1) for sharing plasmids. Drs. Liu and Zhang are from the Department of Pathology, Peking Union Medical College Hospital, Chinese Academy of Medical Sciences and Peking Union Medical College, Tsinghua University, Beijing, PR China. We also thank Dr. Robert M. Lavker for useful discussions.

Grant Support

The National Nature Science Foundation of China (grant 30471970), the National Science and Technology Support Project (the 11th Five-Year Plan) of China (grant 2006BAI02A14), the Scientific Research Special Projects of Health Industry of China (grant 200802011), and Roche Company.

The costs of publication of this article were defrayed in part by the payment of page charges. This article must therefore be hereby marked *advertisement* in accordance with 18 U.S.C. Section 1734 solely to indicate this fact.

Received 12/17/2009; revised 03/29/2010; accepted 05/03/2010; published OnlineFirst 07/06/2010.

References

- Garzon R, Calin GA, Croce CM. MicroRNAs in cancer. *Annu Rev Med* 2009;60:167–79.
- Slack FJ, Weidhaas JB. MicroRNA in cancer prognosis. *N Engl J Med* 2008;359:2720–2.
- Inomata M, Tagawa H, Guo YM, Kameoka Y, Takahashi N, Sawada K. MicroRNA-17-92 down-regulates expression of distinct targets in different B-cell lymphoma subtypes. *Blood* 2009;113:396–402.
- Qian B, Katsaros D, Lu L, et al. High miR-21 expression in breast cancer associated with poor disease-free survival in early stage disease and high TGF- β 1. *Breast Cancer Res Treat* 2009;117:131–40.
- Qi L, Bart J, Tan LP, et al. Expression of miR-21 and its targets (PTEN, PDCD4, TM1) in flat epithelial atypia of the breast in relation to ductal carcinoma *in situ* and invasive carcinoma. *BMC Cancer* 2009;9:163.
- Cimmino A, Calin GA, Fabbri M, et al. miR-15 and miR-16 induce apoptosis by targeting BCL2. *Proc Natl Acad Sci U S A* 2005;102:13944–9.
- Johnson SM, Grosshans H, Shingara J, et al. RAS is regulated by the let-7 microRNA family. *Cell* 2005;120:635–47.
- Iorio MV, Visone R, Di Leva G, et al. MicroRNA signatures in human ovarian cancer. *Cancer Res* 2007;67:8699–707.
- Schepeler T, Reinert JT, Ostenfeld MS, et al. Diagnostic and prognostic microRNAs in stage II colon cancer. *Cancer Res* 2008;68:6416–24.
- Hall A. The cellular functions of small GTP-binding proteins. *Science* 1990;249:635–40.
- Almoguera C, Shibata D, Forrester K, Martin J, Arnheim N, Perucho M. Most human carcinomas of the exocrine pancreas contain mutant c-K-ras genes. *Cell* 1988;53:549–54.
- Rozenblum E, Schutte M, Goggins M, et al. Tumor-suppressive pathways in pancreatic carcinoma. *Cancer Res* 1997;57:1731–4.
- Hingorani SR, Petricoin EF, Maitra A, et al. Preinvasive and invasive ductal pancreatic cancer and its early detection in the mouse. *Cancer Cell* 2003;4:437–50.
- Campbell PM, Groehler AL, Lee KM, Ouellette MM, Khazak V, Der CJ. K-Ras promotes growth transformation and invasion of immortalized human pancreatic cells by Raf and phosphatidylinositol 3-kinase signaling. *Cancer Res* 2007;67:2098–106.
- Kallifatidis G, Rausch V, Baumann B, et al. Sulforaphane targets pancreatic tumour-initiating cells by NF- κ B-induced antiapoptotic signalling. *Gut* 2009;58:949–63.
- Li YY, Popivanova BK, Nagai Y, Ishikura H, Fujii C, Mukaida N. Pim-3, a proto-oncogene with serine/threonine kinase activity, is aberrantly expressed in human pancreatic cancer and phosphorylates bad to block bad-mediated apoptosis in human pancreatic cancer cell lines. *Cancer Res* 2006;66:6741–7.
- McCubrey JA, Steelman LS, Chappell WH, et al. Roles of the Raf/MEK/ERK pathway in cell growth, malignant transformation and drug resistance. *Biochim Biophys Acta* 2007;1773:1263–84.
- Zhang W, Liu HT. MAPK signal pathways in the regulation of cell proliferation in mammalian cells. *Cell Res* 2002;12:9–18.
- Szafrańska AE, Davison TS, John J, et al. MicroRNA expression

- alterations are linked to tumorigenesis and non-neoplastic processes in pancreatic ductal adenocarcinoma. *Oncogene* 2007;26:4442–52.
20. Yu J, Ryan DG, Getsios S, Oliveira-Fernandes M, Fatima A, Lavker RM. MicroRNA-184 antagonizes microRNA-205 to maintain SHIP2 levels in epithelia. *Proc Natl Acad Sci U S A* 2008;105:19300–5.
 21. Aoki K, Yoshida T, Matsumoto N, Ide H, Sugimura T, Terada M. Suppression of Ki-ras p21 levels leading to growth inhibition of pancreatic cancer cell lines with Ki-ras mutation but not those without Ki-ras mutation. *Mol Carcinog* 1997;20:251–8.
 22. Agbunag C, Bar-Sagi D. Oncogenic K-ras drives cell cycle progression and phenotypic conversion of primary pancreatic duct epithelial cells. *Cancer Res* 2004;64:5659–63.
 23. Santos E, Martin-Zanca D, Reddy E, Pierotti M, Della Porta G, Barbacid M. Malignant activation of a K-RAS oncogene in lung carcinoma but not in normal tissue of the same patient. *Science* 1984;223:661–4.
 24. Slebos RJ, Kibbelaar RE, Dalesio O, et al. K-ras oncogene activation as a prognostic marker in adenocarcinoma of the lung. *N Engl J Med* 1990;323:561–5.
 25. Forbes S, Clements J, Dawson E, et al. COSMIC 2005. *Br J Cancer* 2006;94:318–22.
 26. Janssen KP, Alberici P, Fsihi H, et al. APC and oncogenic KRAS are synergistic in enhancing Wnt signaling in intestinal tumor formation and progression. *Gastroenterology* 2006;131:1096–109.
 27. Aguirre AJ, Bardeesy N, Sinha M, et al. Activated Kras and Ink4a/Arf deficiency cooperate to produce metastatic pancreatic ductal adenocarcinoma. *Genes Dev* 2003;17:3112–26.
 28. Castagnola P, Giaretti W. Mutant KRAS, chromosomal instability and prognosis in colorectal cancer. *Biochim Biophys Acta* 2005;1756:115–25.
 29. Lee J, Jang KT, Ki CS, et al. Impact of epidermal growth factor receptor (EGFR) kinase mutations, EGFR gene amplifications, and KRAS mutations on survival of pancreatic adenocarcinoma. *Cancer* 2007;109:1561–9.
 30. Cheng JQ, Ruggeri B, Klein WM, et al. Amplification of AKT2 in human pancreatic cells and inhibition of AKT2 expression and tumorigenicity by antisense RNA. *Proc Natl Acad Sci U S A* 1996; 93:3636–41.
 31. Bondar VM, Sweeney-Gotsch B, Andreeff M, Mills GB, McConkey DJ. Inhibition of the phosphatidylinositol 3'-kinase-AKT pathway induces apoptosis in pancreatic carcinoma cells *in vitro* and *in vivo*. *Mol Cancer Ther* 2002;1:989–97.
 32. Hingorani SR, Wang L, Multani AS, et al. Trp53R172H and KrasG12D cooperate to promote chromosomal instability and widely metastatic pancreatic ductal adenocarcinoma in mice. *Cancer Cell* 2005;7:469–83.
 33. Tanno S, Tanno S, Mitsuuchi Y, Altomare DA, Xiao GH, Testa JR. AKT activation up-regulates insulin-like growth factor I receptor expression and promotes invasiveness of human pancreatic cancer cells. *Cancer Res* 2001;61:589–93.
 34. Wee S, Jagani Z, Xiang KX, et al. PI3K pathway activation mediates resistance to MEK inhibitors in KRAS mutant cancers. *Cancer Res* 2009;69:4286–93.
 35. Seger R, Krebs EG. The MAPK signaling cascade. *FASEB J* 1995;9: 726–35.
 36. Kohno M, Pouyssegur J. Targeting the ERK signaling pathway in cancer therapy. *Ann Med* 2006;38:200–11.
 37. Boucher MJ, Duchesne C, Lainé J, Morisset J, Rivard N. cAMP protection of pancreatic cancer cells against apoptosis induced by ERK inhibition. *Biochem Biophys Res Commun* 2001;285:207–16.
 38. Calin GA, Croce CM. MicroRNA signatures in human cancers. *Nat Rev Cancer* 2006;6:857–66.
 39. Esquela-Kerscher A, Slack FJ. Oncomirs—microRNAs with a role in cancer. *Nat Rev Cancer* 2006;6:259–69.
 40. Guttilla IK, White BA. Coordinate regulation of FOXO1 by miR-27a, miR-96, and miR-182 in breast cancer cells. *J Biol Chem* 2009;284: 23204–16.

Cancer Research

The Journal of Cancer Research (1916–1930) | The American Journal of Cancer (1931–1940)

miRNA-96 Suppresses KRAS and Functions as a Tumor Suppressor Gene in Pancreatic Cancer

Shuangni Yu, Zhaohui Lu, Changzheng Liu, et al.

Cancer Res 2010;70:6015-6025. Published OnlineFirst July 7, 2010.

Updated version	Access the most recent version of this article at: doi: 10.1158/0008-5472.CAN-09-4531
Supplementary Material	Access the most recent supplemental material at: http://cancerres.aacrjournals.org/content/suppl/2010/07/02/0008-5472.CAN-09-4531.DC1

Cited articles	This article cites 40 articles, 19 of which you can access for free at: http://cancerres.aacrjournals.org/content/70/14/6015.full.html#ref-list-1
-----------------------	--

Citing articles	This article has been cited by 18 HighWire-hosted articles. Access the articles at: /content/70/14/6015.full.html#related-urls
------------------------	---

E-mail alerts	Sign up to receive free email-alerts related to this article or journal.
----------------------	--

Reprints and Subscriptions	To order reprints of this article or to subscribe to the journal, contact the AACR Publications Department at pubs@aacr.org .
-----------------------------------	--

Permissions	To request permission to re-use all or part of this article, contact the AACR Publications Department at permissions@aacr.org .
--------------------	---